Jurnal Pijar MIPA
https://jurnalfkip.unram.ac.id/index.php/JPM

ISSN 1907-1744 (Print)
ISSN 2460-1500 (Online)

Adsorption of Rhodamine B Dye Using Concentrated Extract of Secondary Metabolites from Mango Peel (*Mangifera indica* L.)

Habib Al Arasy*, Sri Benti Etika

Department of Chemistry, Faculty of Mathematics and Natural Sciences, Padang State University, Padang, Indonesia
*e-mail: habibalarasy@gmail.com

Received: June 19, 2026. Accepted: August 31, 2026. Published: October 29, 2026

Abstract: Rhodamine B is a synthetic dye widely used in various industrial applications and poses a serious environmental pollution due to its toxicity and resistance to biodegradation. This study aimed to evaluate the adsorption performance of concentrated secondary metabolite extract from mango peel (*Mangifera indica* L.) as a natural adsorbent for the removal of Rhodamine B from aqueous solutions. The effects of pH, initial dye concentration, and contact time on adsorption capacity were investigated. The residual Rhodamine B concentration was determined using UV-Visible spectrophotometry, while the adsorption behavior was evaluated using Langmuir and Freundlich isotherm models as well as pseudo-first-order (PFO) and pseudo-second-order (PSO) kinetic models. Functional group interactions before and after adsorption were characterized using Fourier Transform Infrared (FTIR) spectroscopy. The optimum adsorption conditions were obtained at pH 3, an initial Rhodamine B concentration of 1400 ppm**,** and a contact time of 30 min, resulting in an adsorption capacity of 154.30 mg g^{-1}**.** The adsorption equilibrium was better described by the Langmuir isotherm model ($R^2 = 0.8843$) than by the Freundlich model ($R^2 = 0.6289$), with a maximum adsorption capacity (Qmax) of 161.29 mg g^{-1} and a separation factor (R_L) of 0.062, indicating favorable monolayer adsorption. Kinetic analysis showed that the adsorption process followed the pseudo-second-order model ($R^2 = 0.9991$) rather than the pseudo-first-order model ($R^2 = 0.0843$), suggesting that adsorption predominantly occurred through chemisorption. FTIR analysis further confirmed the involvement of hydroxyl, carbonyl, aromatic, and C-O functional groups in the adsorption process through shifts in characteristic absorption bands after adsorption. These findings demonstrate that concentrated secondary metabolite extract from mango peel is a promising natural adsorbent for Rhodamine B removal and has potential for application in environmentally friendly dye wastewater treatment.

Keywords: Adsorption Kinetics; Biosorbents; Mango Peel; Rhodamine B; Secondary Metabolites.

Introduction

Colored liquid waste from various industries, especially the textile industry, is often discharged without adequate treatment and has become a major cause of serious water pollution. Many dyes used in the textile industry are toxic and non-biodegradable, thereby causing harmful effects on aquatic ecosystems and human health [1]. Textile dyes are chemical compounds with complex, stable structures, generally containing aromatic rings and heteroatoms, including azo, diazo, benzidine, and anthraquinone groups. These structural characteristics make dyes resistant to degradation and hazardous to the environment [2]. One of the hazardous dyes frequently used is Rhodamine B. Rhodamine B is difficult to degrade by microorganisms because its chemical structure contains basic amino groups and a benzene core [3]. The structure of Rhodamine B is shown in Figure 1.

This synthetic dye belongs to the xanthene basic dye class and occurs as an odorless crystalline powder. Rhodamine B solution appears purplish-red at high concentrations and bright red at low concentrations. This dye is toxic and harmful to human health, causing irritation and respiratory disorders if ingested or inhaled. When discharged into aquatic environments, Rhodamine B contaminates water, alters pH conditions, and disrupts microorganisms as well as aquatic organisms [4].

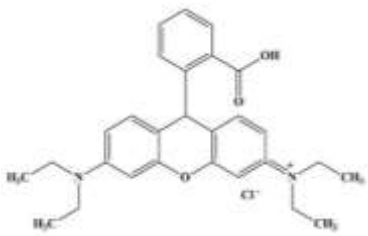


Figure 1. Structure of Rhodamine B

Dye-containing wastewater can be treated using several methods, including coagulation-flocculation and reverse osmosis [3], oxidation processes, ion exchange, ozonation, and adsorption [5]. Among these, adsorption is one of the most widely applied methods because of its high efficiency, operational simplicity, low cost, and low energy requirement [6]. Mechanistically, adsorption is defined as the accumulation of a substance (molecules or ions) on the surface of an adsorbent material [2].

Previous studies by Bahrizal et al. [7] demonstrated that several types of biomass can be used as low-cost adsorbents due to the presence of functional groups such as -COOH, -OH, N-H, C-H, C=O, and C=C. Biomass materials that have been utilized as adsorbents include langsat peel, cassava peel waste [8], kepok banana peel waste [9], lime peel [10], and mango peel [11]. In addition, several studies

How to Cite:
H. A. Arasy and S. B. Etika, "Adsorption of Rhodamine B dye using concentrated extract of secondary metabolites from mango peel (*Mangifera indica* L.)," *J. Pijar MIPA*, vol. 21, no. 5, pp. 1039–1049, Oct. 2026. https://doi.org/10.29303/jpm.v21i5.12521

have reported the use of biomass extracts, such as vernonia leaf extract [12], gambier leaf extract [13], and rambutan peel flavonoid extract [14].

One potential adsorbent for dye removal is secondary metabolites. These compounds are produced through plant metabolic processes and are rich in active functional groups, enabling them to bind dye molecules effectively. Sridevitri & Etika [15] reported the use of rambutan peel secondary metabolites for the adsorption of Methylene Blue using the batch method, achieving an adsorption capacity of 10.9669 mg g^{-1}. Rambutan peel for the adsorption of Rhodamine B with a capacity of 21.5945 mg g^{-1} [14]. Based on the successful utilization of rambutan peel waste, other plant materials with similar characteristics may also be promising, one of which is mango.

Mango belongs to the genus Mangifera, with the species Mangifera indica L., which originated in India before spreading to various regions, including Indonesia [16]. Mango is a popular fruit widely favored in Indonesia because of its sweet taste. Besides the fruit, all parts of the mango plant have health benefits and medicinal potential due to the presence of secondary metabolites [17,18]. Currently, people mainly utilize the pulp, while the peel is often discarded as household waste [19]. Research by Kim et al. [20] showed that mango peel contains higher total polyphenol content than the fruit pulp. According to data from Badan Pusat Statistik [21], national mango production reached approximately 3.6 million tons in 2024, generating around 574.000 tons of mango peel annually.

Mango peel contains abundant secondary metabolites, including flavonoids, saponins, tannins, alkaloids, terpenoids, and steroids, making it a promising material for Rhodamine B adsorption. These secondary metabolites may participate in several adsorption mechanisms, including hydrogen bonding, Van der Waals interactions, electrostatic interactions, and π–π interactions [22]. Patra & Mishra [23] mainly focused on converting mango peel into activated carbon or modified adsorbents through chemical or thermal activation. However, studies investigating the direct use of concentrated secondary metabolite extract from mango peel as a biosorbent for Rhodamine B adsorption remain very limited. Previous studies have predominantly utilized mango peel in the form of raw biomass, modified biomass, or activated carbon for pollutant removal. These approaches primarily rely on lignocellulosic components, such as cellulose, hemicellulose, and lignin, as the main adsorption matrix [24]. Although these materials have demonstrated satisfactory adsorption performance, the extraction and direct utilization of secondary metabolites remain largely unexplored.

In contrast, concentrated secondary metabolite extracts are expected to provide a higher density of chemically active compounds, including phenolics, flavonoids, mangiferin, tannins, and other oxygen-containing metabolites. These compounds contain abundant hydroxyl, carbonyl, and aromatic functional groups that can directly participate in hydrogen bonding, π–π interactions, and electrostatic interactions with dye molecules. Therefore, the use of concentrated secondary metabolite extracts is expected to provide a more specific adsorption mechanism than conventional biomass, whose adsorption is predominantly governed by the lignocellulosic matrix.

To the best of our knowledge, studies investigating Rhodamine B adsorption using concentrated secondary metabolite extracts directly isolated from mango peel remain very limited. Therefore, this study utilized concentrated secondary metabolite extract obtained from Arumanis mango peel (*Mangifera indica* cv. Arumanis) to evaluate their adsorption performance for Rhodamine B. This work is expected to provide a new strategy for the valorization of mango peel waste as an environmentally friendly biosorbent while improving the understanding of the adsorption mechanism governed by plant secondary metabolites.

Based on this background, the present study utilized mango peel as a biosorbent. The mango peel used was the Arumanis cultivar (*Mangifera indica* cv. Arumanis) because of its abundant availability as local waste. In addition to its abundance, the Arumanis cultivar has also been reported to possess relatively high total phenolic content compared with other cultivars, making it a potential source of active compounds for adsorption purposes [25]. Preliminary phytochemical screening of the sample confirmed the presence of flavonoids, alkaloids, saponins, and tannins, while steroids tested negative. The presence of these compounds indicates functional groups such as hydroxyl (-OH), carbonyl (C=O), and amine ($-NH_2$), which serve as binding sites for dye molecules. Therefore, this study aimed to evaluate the adsorption performance of concentrated secondary metabolite extract from mango peel toward Rhodamine B through batch adsorption experiments, equilibrium isotherm analysis, adsorption kinetics, and FTIR characterization to elucidate the adsorption mechanism.

Research Methods

Materials and Instrumentation

The materials used in this study were mango peel, distilled methanol, distilled ethyl acetate, distilled n-hexane, Rhodamine B dye solution, distilled water, nitric acid (HNO_3) and sodium hydroxide (NaOH), both from Merck. For characterization, the instruments utilized included a Fourier Transform Infrared (FTIR) Spectrophotometer (Perkin Elmer) and a UV-Vis Spectrophotometer (Genesys 30).

Sample Preparation

The mango peel was washed under running water, cut into small pieces, and then air-dried at room temperature until completely dry. The dried samples were then used for preliminary phytochemical analysis to determine the content of secondary metabolites, including alkaloids, flavonoids, saponins, tannins, terpenoids, and steroids.

Extraction and Fractionation

A total of 1.5 kg of dried sample, previously cut into small pieces, was macerated in methanol until the sample tested negative for secondary metabolites by phytochemical tests. The solvent was then filtered off and the residue was evaporated using a rotary evaporator to obtain a concentrated extract. The concentrated extract was subsequently mixed with distilled water at 45°C to produce an aqueous extract. The aqueous extract was fractionated using a separatory

funnel with n-hexane as solvent. This process was repeated until the n-hexane layer became clear and phytochemical tests showed negative results for secondary metabolites. Two fractions were obtained, namely the aqueous fraction and the n-hexane fraction. The aqueous fraction was then repeatedly fractionated with ethyl acetate. The ethyl acetate fraction obtained was concentrated using a rotary evaporator to produce a viscous extract rich in secondary metabolites, which was then characterized by FTIR spectroscopy [14].

Effect of pH

A total of 25 mL of a Rhodamine B solution with a concentration of 50 ppm was treated by adjusting the pH using HNO_3 or NaOH until it reached a pH level of 2-7. Each of these solutions was then mixed with 0.2 grams of concentrated mango peel extract in a shaker at 200 rpm for 60 minutes using a batch method, and the resulting filtrate was collected. The concentration of unabsorbed Rhodamine B was measured using a UV-Vis spectrophotometer at the maximum wavelength obtained to determine the optimum pH.

Effect of Contact Time

A total of 0.2 grams of concentrated secondary metabolite extract from mango peel was weighed and mixed with 25 mL of Rhodamine B solution at the optimum pH and concentration. The solutions were then brought into contact using a batch system and shaken at 200 rpm for 15, 30, 45, 60, and 75 minutes. The solutions were then filtered, and the filtrates were collected. The filtrate was measured for the concentration of unabsorbed Rhodamine B at the maximum wavelength using a UV-Vis spectrophotometer to determine the optimal contact time.

Results and Discussion

Phytochemical Screening

Phytochemical screening is a qualitative test conducted to determine the content of secondary metabolites in a sample. The secondary metabolites tested include flavonoids, alkaloids, terpenoids, steroids, tannins, and saponins. Preliminary test results for secondary metabolites from mango peels are shown in Table 1.

Table 1. Results of Phytochemical Screening of Secondary Metabolite Compounds in Mango Peels

Secondary Metabolites	Reagents	Results
Flavonoids	NaOH 10%	+
Alkaloids	Mayer	+
	Wagner	+
	Dragendorff	+
Terpenoids	Salkwoski	-
Steroid	Lieberman-burchad	-
Tannin	$FeCl_3$ 1%	+
Saponin	H_2O	+

Phytochemical screening showed that mango peel contains flavonoids, alkaloids, tannins, and saponins. This is consistent with research conducted by Noviyanty et al. [26] and Anggraeni et al. [27] that showed mango peel contains secondary metabolites including flavonoids, alkaloids, tannins, and saponins.

Extraction and Fractionation

The cleaned mango peel samples were cut into small pieces and air-dried at room temperature to prevent degradation of thermolabile compounds and to increase the solvent contact surface area, thus improving extraction efficiency [28]. A total of 1.5 kg of dried crude drug was macerated using distilled methanol. Maceration was chosen due to its simplicity and the absence of heat, making it suitable for temperature-sensitive compounds. Distilled methanol was used to ensure solvent purity and minimize interference during extraction and subsequent analysis. Its high polarity allows for effective extraction of secondary metabolites such as flavonoids, tannins, and phenolic compounds, often resulting in higher phenolic and flavonoid contents compared to other solvents [29].

The maceration process was carried out for 3 x 24 hours until the residue tested negative for secondary metabolites. This method is based on diffusion, where solvents penetrate plant cells and dissolve compounds with similar polarity, driven by differences in osmotic pressure [30]. The extract was then concentrated using a rotary evaporator under reduced pressure to remove methanol and obtain a viscous extract while preventing thermal degradation [31]. The resulting 247.9 g of extract was redissolved in 150 mL of warm water at 45°C to increase the solubility of polar compounds.

The aqueous extract was then fractionated based on polarity using the principle of "like dissolves in like" [32]. Sequential partitioning with *n*-hexane was repeated five times to remove non-polar compounds until the organic layer became clear. The remaining aqueous phase was then fractionated with ethyl acetate, a process repeated 5 times to extract semi-polar compounds. This stepwise fractionation ensured optimal separation of metabolites by polarity, yielding an ethyl acetate fraction rich in secondary metabolites.

Fourier Transform Infrared Spectra Analysis

Based on the FTIR spectrum, several absorption peaks were observed, indicating the presence of functional groups of secondary metabolites in the extract. The broad peak at 3332 cm^{-1} indicates the presence of O-H groups, typically associated with phenolic compounds such as flavonoids and tannins. Then, the peak at 2990 cm^{-1} indicates the presence of aliphatic C-H groups, indicating hydrocarbon chains in the compound's structure. The strong peak at 1701 cm^{-1} indicates the presence of C=O (carbonyl) groups, which originate from carboxylic acids, esters, or their derivatives. Meanwhile, the peak at 1608 cm^{-1} indicates the presence of aromatic C=C bonds characteristic of phenolic compounds. The absorption at 1532 cm^{-1} likely originates from N-H groups or aromatic ring vibrations, which indicates the presence of alkaloid compounds. The peak at 1445 cm^{-1} indicates C-H bending, supporting the presence of organic structures. In the fingerprint region (1312-1026 cm^{-1}), several peaks are visible, indicating the presence of C-O and C-O-C groups, which are commonly found in flavonoids,

saponins, and tannins. The peaks at 947 cm^{-1} and 869 cm^{-1} indicate aromatic C-H vibrations, which further strengthen the presence of aromatic rings in the extract. The FTIR results obtained in this study are consistent with the research by Ibrahim et al. [33] on mango peel extract, which also showed the presence of major functional groups such as -OH, C=O, and C=C, characteristic of secondary metabolites. The FTIR spectrum is shown in Figure 2.

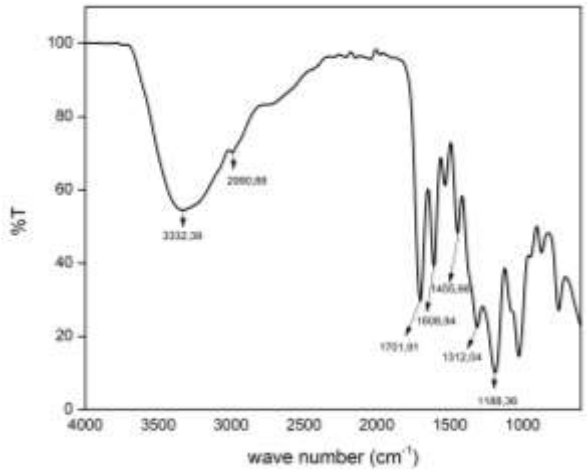


Figure 2. FTIR spectrum of the concentrated extract of secondary metabolite compounds of mango peel

Standard Curve Preparation of Rhodamine B

Prior to constructing the calibration curve, the maximum absorption wavelength (λmax) of Rhodamine B was determined using a UV-Vis spectrophotometer. The maximum absorbance was observed at 554 nm, which was subsequently used as the analytical wavelength for all quantitative measurements because it provides the highest sensitivity and accuracy. The accuracy of the Rhodamine B concentration analysis was ensured by creating a calibration curve prior to determining the optimal conditions. The phenomenon of increasing absorbance proportional to the concentration confirmed compliance with the Lambert-Beer law [34]. The superior linearity was demonstrated by the regression equation y = 0.1272x + 0.0198, with an R2 of 0.9996, as shown in Figure 3.

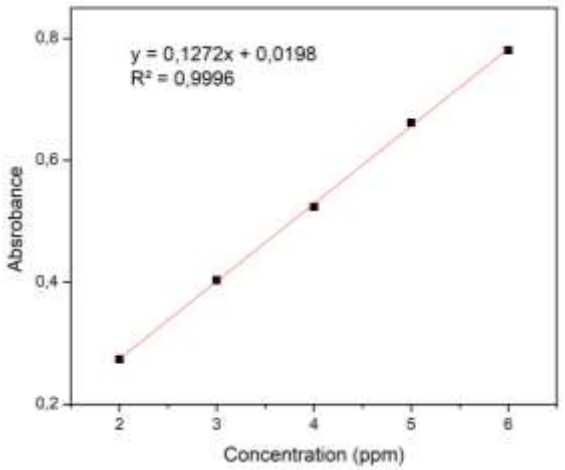


Figure 3. Preparation of Rhodamine B Calibration Curve

Effect of Optimum pH of Rhodamine B on Secondary Metabolite Extract

Solution pH is a critical factor influencing the adsorption process, as it affects the surface charge of the adsorbent, the dissociation of functional groups, and the adsorption capacity [35]. In this study, the optimum pH for Rhodamine B adsorption was evaluated over a pH range of 2-7. The adsorption capacity increased from 4.5244 mg g^{-1} at pH 2 to a maximum of 5.3065 mg g^{-1} at pH 3, and subsequently decreased to 3.8980 mg g^{-1} at pH 7, indicating that the optimum adsorption occurred at pH 3, as seen in Figure 4.

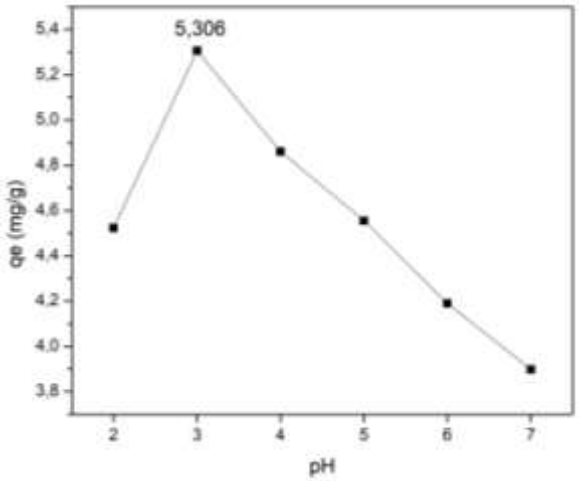


Figure 4. pH Curve of Rhodamine B Against a Concentrated Extract of Secondary Metabolites

At pH 2, the high concentration of H^+ ions protonates functional groups on the adsorbent surface, rendering it positively charged and repelling the cationic Rhodamine B, thereby reducing adsorption efficiency. As the pH increases to 3, partial deprotonation of functional groups such as carboxyl and hydroxyl groups generates negative charges, enhancing electrostatic attraction with Rhodamine B and leading to maximum adsorption capacity. Additionally, hydrogen bonding and π–π interactions between the aromatic structure of Rhodamine B and secondary metabolites may contribute to adsorption [36]. At higher pH values (4-7), the adsorption capacity decreases due to changes in the amphoteric form of Rhodamine B and increased competition from OH^- ions for active sites [37].

These results indicate that acidic conditions are optimal for Rhodamine B adsorption, consistent with previous findings by Oyekanmi et al. [38], who also reported an optimum pH of 3. Under these conditions, a favorable balance between adsorbent surface charge and Rhodamine B speciation enhances adsorption through electrostatic interactions as well as hydrogen bonding and π–π interactions.

Effect of Contact Time of Rhodamine B on Secondary Metabolite Extract

Determining the optimum contact time aims to determine the time required for the adsorption process to reach maximum capacity before equilibrium is reached. In this study, contact times varied for 15, 30, 45, 60, and 75 minutes at an optimum pH of 3 and an optimum Rhodamine

B concentration of 1400 ppm. The effect of contact time on Rhodamine B dye absorption is shown in Figure 5.

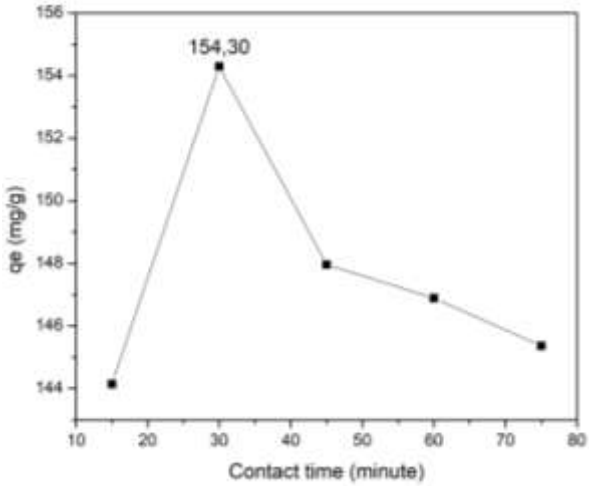


Figure 5. Contact Time Curve of Rhodamine B Against a Concentrated Extract of Secondary Metabolites

The results showed that the adsorption capacity increased from 144.13 mg g^{-1} at 15 minutes to 154.30 mg g-1 at 30 minutes. This increase indicates that during the initial stage of adsorption, many active sites remained on the surface of the concentrated extract of mango peel secondary metabolites, allowing Rhodamine B molecules to readily interact and occupy them. Furthermore, the concentration difference between the solution and the adsorbent surface remains large, resulting in a strong mass-transfer driving force. Consequently, the adsorption rate is rapid at the beginning of the process.

Dye adsorption generally proceeds very rapidly at the beginning of the process due to the large number of unoccupied active sites on the adsorbent [39]. After 30 minutes of contact time, the adsorption capacity gradually decreased to 145.36 mg g-1 by 75 minutes. This indicates that the system has approached adsorption equilibrium. At this point, most of the active sites are occupied by Rhodamine B molecules, resulting in a decreased adsorption rate. Furthermore, the increasing number of Rhodamine B molecules adsorbed on the surface can create electrostatic barriers and repulsive forces between adsorbate molecules occupying adjacent sites, thereby reducing adsorption effectiveness at longer contact times. A similar phenomenon was reported by Thakur & Kaur [40] and research by Caglar & Kayranli [41], which stated that after equilibrium was reached, increasing the contact time no longer increased the adsorption capacity because most of the active sites had been filled and dynamic adsorption–desorption equilibrium occurred.

Adsorption Isotherms

Adsorption isotherm analysis was conducted to determine the characteristics of the interaction between Rhodamine B molecules and the adsorbent surface, and to determine the most appropriate adsorption model to describe the adsorption process [42]. This study employed two isotherm models commonly used in adsorption studies: the Langmuir and the Freundlich isotherms. The suitability of the two models was determined using the coefficient of determination (R^2) from the linear regression of each isotherm equation.

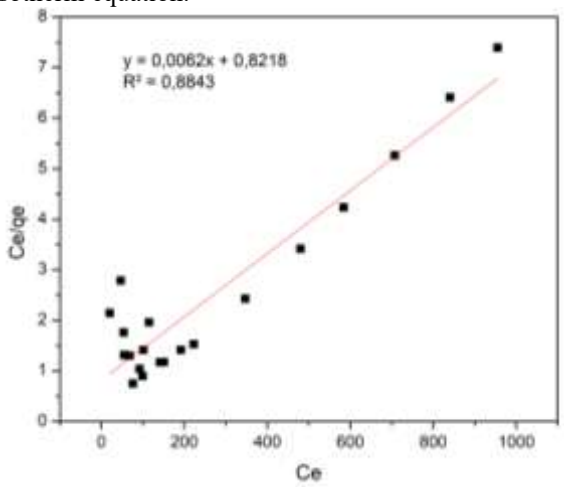


Figure 6. Langmuir isotherm model graph

The Langmuir isotherm model assumes that adsorption occurs on a homogeneous adsorbent surface with a limited number of active sites. Each active site can only be occupied by one adsorbate molecule, forming a monolayer [43]. In the Langmuir isotherm model, Ce represents the equilibrium adsorbate concentration (mg L^{-1}), and K_L indicates the affinity between the adsorbent and the adsorbate. A positive K_L value indicates a favorable interaction between Rhodamine B and the adsorbent. An important characteristic of the Langmuir isotherm can be expressed by a dimensionless constant called the separation factor (R_L), which is used to determine whether an adsorption process is favorable or unfavorable [44]. The Langmuir isotherm analysis yielded a coefficient of determination (R^2) of 0.8843, as shown in Figure 6.

The Freundlich isotherm model is used to describe adsorption on heterogeneous surfaces. This model assumes that the adsorption energy at each active site varies, allowing adsorption to occur in more than one layer (multilayer). In this process, active sites with higher affinity are occupied first before adsorbate molecules occupy other active sites with lower energy [43]. In this model, the constant K_F indicates the estimated adsorption capacity, and the value of n describes the adsorption intensity [45]. The Freundlich isotherm model graph is shown in Figure 7.

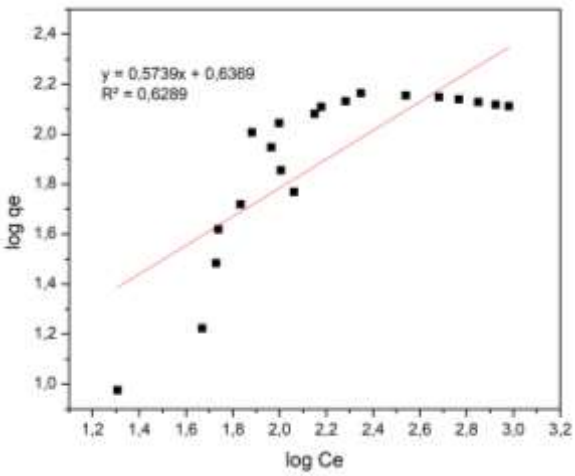


Figure 7. Freundlich isotherm model graph

Based on the adsorption isotherm analysis, the Langmuir isotherm model yielded a higher coefficient of determination (R^2) of 0.8843 and a maximum adsorption capacity of 161.29 mg g^{-1}, while the Freundlich isotherm model yielded an R^2 of 0.6289. The higher R^2 value in the Langmuir model indicates that the adsorption of Rhodamine B by the concentrated extract of mango peel secondary metabolites is better explained by the Langmuir model than by the Freundlich model. These results indicate that the adsorption process tends to occur at relatively homogeneous active sites, forming a monolayer on the adsorbent surface. The Langmuir model obtained a Langmuir constant K_L of 0.00754 L mg^{-1}, indicating an affinity between the adsorbent and adsorbate, and a separation factor (R_L) of 0.062. R_L values in the range $0 < R_L < 1$ indicate that the Rhodamine B adsorption process is favorable [44]. Meanwhile, the Freundlich model produced an adsorption constant (K_F) of 4.33 mg g^{-1} and an adsorption intensity (n) of 1.74. The n value in the range of 1-10 indicates that adsorption proceeds well and the adsorbent has a fairly high affinity for the adsorbate.

Based on these results, the concentrated extract of secondary metabolites of mango peel showed good adsorption capacity towards Rhodamine B. To assess the performance of the adsorbent used, the adsorption capacity in this study was compared with those of several previously reported biomass-based adsorbents.

Table 2. Comparison of the adsorption capacity of mango peel secondary metabolite extracts with several other adsorbents

Adsorbent	Adsorbate	Qmax (mg g^{-1})	Reference
Banana peel	Rhodamine B	20.6	[46]
Orange peel	Rhodamine B	14.3	[46]
Trapa natans shell	Rhodamine B	136.46	[47]
Rambutan peel	Rhodamine B	21.59	[14]

Table 2 shows that the adsorption capacity obtained in this study is comparable to or higher than several biomass-based adsorbents previously reported for Rhodamine B removal. Although some chemically modified adsorbents exhibit higher adsorption capacities due to increased surface area and porosity, the concentrated secondary metabolite extract used in this study achieved a relatively high adsorption capacity without chemical activation. This performance is attributed to the abundance of phenolic compounds, particularly mangiferin, gallic acid, and quercetin, which provide numerous hydroxyl, carbonyl, and aromatic functional groups that interact with Rhodamine B molecules.

Adsorption kinetic

Adsorption kinetics is an important aspect of adsorption research because it provides information about the rate of adsorbate absorption by the adsorbent and the mechanisms that control the adsorption process. In contrast to isotherm studies that describe the relationship between adsorption capacity and adsorbate concentration at equilibrium, kinetics studies explain the change in adsorption capacity over time until equilibrium is reached [48]. In this study, kinetic analysis was carried out using the pseudo-first-order (PFO) and pseudo-second-order (PSO) models to evaluate the suitability of the kinetic models and to obtain an overview of the adsorption mechanism of Rhodamine B by concentrated extracts of secondary metabolites from mango peel.

The Pseudo-first-order (PFO) model developed by Lagergren assumes that the adsorption rate is proportional to the number of active sites remaining available on the adsorbent surface. This model is generally used to describe the initial stages of adsorption and is often associated with processes dominated by mass transfer or external diffusion. The linear equation is expressed as:

$$\ln(qe - qt) = \ln qe - k_1 t$$

Where qe is the adsorption capacity at equilibrium (mg g^{-1}), qt is the adsorption capacity at time t, and k_1 is the pseudo-first-order rate constant ($minute^{-1}$). The suitability of this model is generally evaluated based on the coefficient of determination (R^2) and the agreement between the calculated qe value and the experimental qe value. The Pseudo-second-order (PSO) model developed by Ho and McKay assumes that the adsorption rate depends on the square of the number of unoccupied active sites. This model is widely used in adsorption research because it often provides a better fit to experimental data than the PFO model. The linear PSO equation is expressed as:

$$\frac{t}{qt} = \frac{1}{k_2 q_e^2} + \frac{t}{qe}$$

where k_2 is the pseudo-second-order rate constant ($g.mg^{-1}.min^{-1}$). Based on the adsorption kinetics analysis, the pseudo-first-order (PFO) model produced a coefficient of determination (R^2) of 0.0843, while the pseudo-second-order (PSO) model produced an R^2 of 0.9991. The linear plots obtained from the PFO and PSO kinetic models are presented in Figure 8 (a) and Figure 8 (b), respectively. These plots were used to evaluate the suitability of each kinetic model for describing the adsorption process of Rhodamine B by the concentrated secondary metabolite extract of mango peel.

The significantly higher coefficient of determination for the PSO model indicates a much better fit to the experimental data than the PFO model. Thus, the adsorption kinetics of Rhodamine B by concentrated extracts of mango peel secondary metabolites more closely follow the pseudo-second-order model. The low R^2 value in the PFO model indicates that the adsorption rate is not solely influenced by the number of vacant active sites on the adsorbent surface, as assumed in the model. This indicates that the PFO model cannot describe the adsorption kinetics of Rhodamine B in this study. The PFO model is generally used to describe adsorption processes that occur through physisorption mechanisms, namely, relatively weak interactions such as Van der Waals forces or molecular diffusion toward the adsorbent surface [49].

In contrast, the Pseudo-second-order (PSO) model showed an R^2 value of 0.9991, indicating good agreement with the experimental data. The high coefficient of determination indicates that the adsorption rate is more influenced by the interaction between the adsorbent and the

adsorbate than by diffusion alone towards the adsorbent surface. In many adsorption studies, the PSO model is often associated with the chemisorption mechanism, an adsorption process involving stronger interactions between active functional groups on the adsorbent and adsorbate molecules through electron exchange or sharing. Therefore, the high fit of the PSO model in this study indicates that Rhodamine B adsorption likely occurs via chemisorption [50].

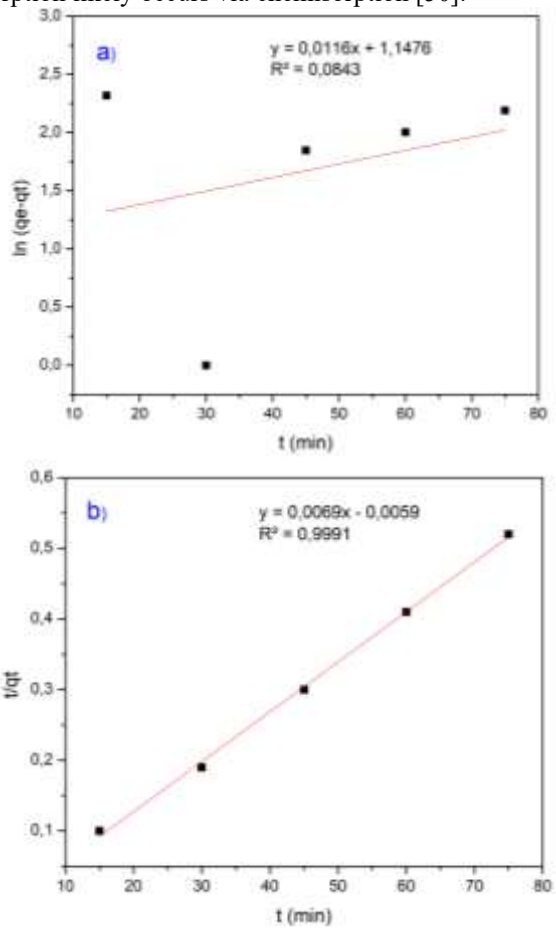


Figure 8. (a) Linear plot of the pseudo-first-order kinetic model and (b) linear plot of the pseudo-second-order kinetic model for Rhodamine B adsorption onto concentrated secondary metabolite extracts of mango peel

Mechanism of Adsorption

The decrease in Rhodamine B concentration after the adsorption process indicates an interaction between the dye molecules and the secondary metabolites contained in the mango peel extract. This interaction causes Rhodamine B molecules to bind to the adsorbent's active sites, reducing the amount of dye remaining in solution, as evidenced by a decrease in dye intensity. Among the identified secondary metabolites, phenolic compounds represented by mangiferin, gallic acid, and quercetin are considered to contribute most significantly to Rhodamine B adsorption because of their abundant hydroxyl and aromatic functional groups. Nevertheless, other classes of secondary metabolites, including flavonoids, alkaloids, tannins, and saponins, may also participate in the adsorption process through the presence of hydroxyl, carbonyl, amine, and other oxygen-containing functional groups capable of interacting with Rhodamine B molecules. This finding aligns with research conducted by Oyekanmi et al. [38] that found a similar mechanism for the adsorption of Rhodamine B dye using banana peel as an adsorbent.

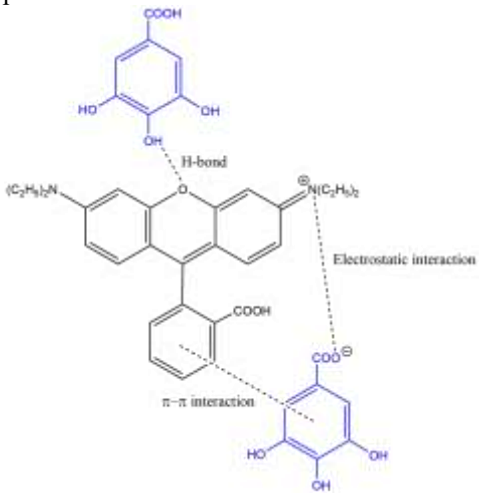


Figure 9. Mechanism of interaction between metabolite extract (Gallic Acid) and Rhodamine B dye

The interaction mechanism that occurred in this study is shown in Figure 9. Phenolic compounds such as gallic acid, which have hydroxyl and carboxylic groups found in secondary metabolites, have the potential to form hydrogen bonds with oxygen atoms and amine groups in Rhodamine B molecules. Furthermore, deprotonated carboxylic groups (-COO⁻) can interact with the positively charged center in the Rhodamine B structure through electrostatic forces. This interaction causes Rhodamine B molecules to be adsorbed on the adsorbent surface and reduces its concentration in solution. Furthermore, the presence of aromatic rings in phenolic and flavonoid compounds allows for π–π interactions with Rhodamine B's xanthene aromatic ring system. Kainth et al. [34] reported that a combination of hydrogen bonds, electrostatic interactions, and π–π interactions is the main mechanism contributing to Rhodamine B adsorption on adsorbents rich in oxygen functional groups.

To verify the proposed adsorption mechanism, FTIR spectroscopy was employed to identify changes in the functional groups of the concentrated secondary metabolite extract before and after adsorption. The resulting spectra are presented in Figure 10.

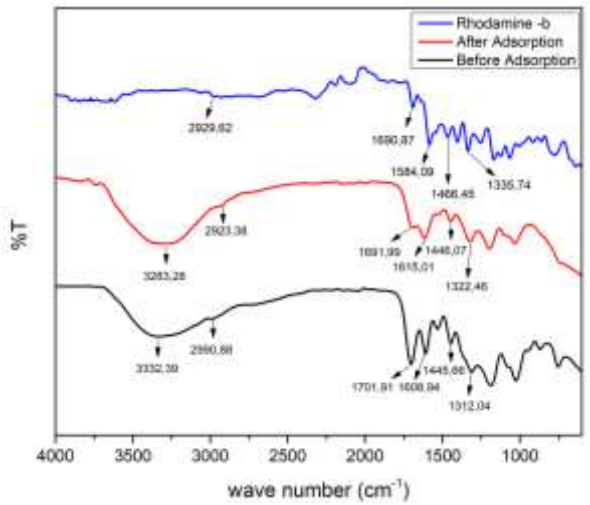


Figure 10. FTIR spectrum of concentrated extract of secondary metabolites before and after contact, and Rhodamine B

Based on the FTIR spectrum in Figure 10, changes in wavenumber and absorption intensity after the adsorption process indicate that the chemical environment of the functional groups changes upon interaction with Rhodamine B molecules. Before adsorption, the extract shows absorption bands at 3332.39 cm^{-1} (O–H), 2990.88 cm^{-1} (aliphatic C–H), 1701.91 cm^{-1} (C=O), 1608.94 cm^{-1} (aromatic C=C), as well as 1455.66 cm^{-1} and 1312.04 $cm^{-1,}$ which are included in the C-H and C-O groups. The presence of these groups indicates active sites that can interact with Rhodamine B molecules. After adsorption, several absorption bands shifted, namely O-H from 3332.39 cm^{-1} to 3283.28 cm^{-1}, aliphatic C-H from 2990.88 cm^{-1} to 2923.38 cm^{-1}, C=O from 1701.91 cm^{-1} to 1691.99 cm^{-1}, aromatic C=C from 1608.94 cm^{-1} to 1615.01 cm^{-1}, and C-O from 1312.04 cm^{-1} to 1322.46 cm^{-1}. These shifts indicate that hydroxyl, carbonyl, aromatic, and C-O groups are involved in the adsorption process through changes in their chemical environment resulting from interactions between the adsorbent and adsorbate [51]. When compared with the spectrum of pure Rhodamine B, there are characteristic bands at 2929.62 cm^{-1} (C-H stretching), 1690.87 cm^{-1} (C=O), 1584.09 cm^{-1} (C=C aromatic), 1466.45 cm^{-1}, and 1335.74 cm^{-1} associated with the C-H and C-N groups. After adsorption, the bands in the adsorbed extract are characteristic of Rhodamine B, particularly at 1691.99 cm^{-1}, 1615.01 cm^{-1}, and 1322.46 cm^{-1}. A comparison of wavenumbers for concentrated secondary metabolite extracts of mango peel before and after adsorption, and pure Rhodamine B, is shown in Table 3.

Table 3. Comparison of FTIR wave numbers of concentrated extract of secondary metabolites of mango peel before adsorption, extract after adsorption, and Rhodamine B

Functional Group	Before Adsorption (cm^{-1})	After Adsorption (cm^{-1})	Rhodamine B (cm^{-1})
O-H stretching	3332.39	3283.28	-
C-H stetching	2990.88	2923.38	2929.62
C=O stretching	1701.91	1691.99	1690.87
C=C aromatik	1608.94	1615.01	1584.09
C-H bending	1455.66	1446.07	1466.45
C-N stretching	1312.04	1322.46	1335.74

Overall, the comparison of FTIR spectra before and after adsorption demonstrates that the functional groups present in the concentrated secondary metabolite extract actively participated in the adsorption of Rhodamine B. The shifts observed in the O-H, C=O, aromatic C=C, and C-O absorption bands, together with the similarity of several absorption regions to those of pure Rhodamine B, indicate that adsorption occurred through multiple interactions involving hydrogen bonding, π–π interactions, and electrostatic attractions. These findings are consistent with the proposed adsorption mechanism and support the excellent agreement of the pseudo-second-order kinetic model, suggesting that the adsorption process tends to proceed through chemisorption.

Study Limitations

Although this study successfully demonstrated the potential of concentrated secondary metabolite extracts from mango peels as a natural adsorbent for Rhodamine B removal, several limitations warrant acknowledgement. The adsorption experiments were conducted without experimental replication; therefore, statistical parameters could not be determined. Nevertheless, all adsorption experiments were conducted under identical experimental conditions and analytical procedures to ensure data consistency. Future studies are recommended to conduct three adsorption experiments and incorporate appropriate statistical analysis to improve the reliability and reproducibility of the findings. Furthermore, additional investigations on adsorbent regeneration and performance evaluation using real textile wastewater are recommended to further assess the practical application of concentrated secondary metabolite extracts.

Conclusion

This study showed that concentrated secondary metabolite extract from mango peel is an effective natural adsorbent for the removal of Rhodamine B. The optimum adsorption conditions were obtained at pH 3, an initial Rhodamine B concentration of 1400 ppm, and a contact time of 30 min, resulting in an adsorption capacity of 154.30 mg/g. The adsorption process was better described by the Langmuir isotherm model ($R^2 = 0.8843$) than the Freundlich model ($R^2 = 0.6289$), with a maximum adsorption capacity (Qmax) of 161.29 mg g^{-1}, indicating favorable monolayer adsorption. Kinetic analysis showed that the adsorption followed the pseudo-second-order (PSO) model ($R^2 = 0.9991$) rather than the pseudo-first-order (PFO) model ($R^2 = 0.0843$), indicating that chemisorption was more dominant. This interpretation is supported by FTIR analysis, which revealed the involvement of O-H, C=O, aromatic C=C, and C-O functional groups in the adsorption process. Overall, these findings indicate that concentrated secondary metabolite extracts from mango peels have promising potential as environmentally friendly biosorbents for Rhodamine B removal. Further studies are recommended to include experimental replication, statistical analysis, adsorbent regeneration, and evaluation using real textile wastewater.

Author's Contribution

H.A. Arasy: responsible for conceptualization, methodology, investigation, data collection, data analysis, interpretation of results, and manuscript preparation. S.B. Etika: contributed to research supervision, provided scientific guidance, reviewed the methodology and results, and contributed to the manuscript's improvement. Both authors approved the final version of the manuscript.

Acknowledgements

The author would like to express sincere gratitude to Sri Benti Etika for her invaluable guidance, encouragement, constructive suggestions, and continuous support throughout

the completion of this research. The author also thanks the lecturers, laboratory staff, and all parties who contributed directly or indirectly to this study. Appreciation is extended to the Department of Chemistry and the laboratory facilities that supported the successful completion of this research.

References

[1] T. A. Khan, S. Sharma, and I. Ali, "Adsorption of Rhodamine B Dye from Aqueous Solution onto Acid Activated Mango (Magnifera indica) Leaf Powder : Equilibrium , kinetic and thermodynamic studies," *J. Toxicol. Environ. Heal. Sci.*, vol. 3, no. 10, pp. 286–297, 2011, doi: http://www.academicjournals.org/JTEHS.

[2] S. Oko, Harjanto, A. Kurniawan, and C. Winanti, "Penurunan Kadar Zat Warna Remazol Brilliant Blue R Dengan Metode Adsorpsi Menggunakan Serbuk CaCO3 Dari Cangkang Telur Dan Karbon Aktif," *Metana Media Komun. Rekayasa Proses dan Teknol. Tepat Guna*, vol. 18, no. 1, pp. 39–45, 2022, doi: 10.14710/metana.v18i1.45766.

[3] Setiyanto, I. Riwayati, and L. Kurniasari, "Adsorpsi Pewarna Tekstil Rodhamin B Menggunakan Senyawa Xanthat Pulpa Kopi," *J. Momentum*, vol. 11, no. 1, pp. 24–28, 2015, doi: https://doi.org/10.36499/jim.v11i1.1078.

[4] N. Syakir, D. Oktaviani, and Fitrilawati, "Pengaruh Waktu dan Dosis terhadap Efektivitas Adsorpsi Rhodamine B Oleh Graphene Oxide," *J. Mater. dan Energi Indones.*, vol. 13, no. 02, pp. 45–52, 2023, doi: https://doi.org/10.24198/jme.v13i2.

[5] V. I. Mabayo and R. Orale, "Agricultural-based Biomass as an Efficient Adsorbent in the Removal of Dyes in Dye-contaminated Wastewater : A Mini Review," *Curr. Appl. Sci. Technol.*, vol. 24, no. 1, pp. 1–18, 2024, doi: https://doi.org/10.55003/cast.2023.257011.

[6] S. F. Zahro and S. Adityosulindro, "Literature Review : Penggunaan Bahan Berbasis Limbah Sebagai Adsorben untuk Degradasi Zat Warna pada Air Limbah," *J. Kesehat. Lingkung. Indones.*, vol. 22, no. 3, pp. 359–368, 2023, doi: 10.14710/jkli.22.3.359-368.

[7] Bahrizal, F. Adella, and D. Kurniawati, "Adsorption of Rhodamine B from Aqueous Solution Using Langsat (Lansium domesticum) Shell Powder," *Adv. Biol. Sci. Res.*, vol. 10, pp. 273–276, 2020, doi: https://doi.org/10.2991/absr.k.200807.054.

[8] H. Irawati, N. H. Aprilita, and E. Sugiharto, "Adsorpsi Zat Warna Kristal Violet Menggunakan Limbah Kulit Singkong (Manihot esculenta)," *J. Berk. MIPA*, vol. 25, no. 1, pp. 17–31, 2018, doi: ISSN 0215-9309.

[9] Musafira, N. M. Adam, and D. J. Puspitasari, "Pemanfaatan Limbah Kulit Buah Pisang Kepok (Musa paradisiaca) sebagai Biosorben Zat Warna Rhodamin B," *KOVALEN J. Ris. Kim.*, vol. 5, no. 3, pp. 308–314, 2019, doi: https://doi.org/10.22487/kovalen.2019.v5.i3.14629.

[10] R. A. Kristanti, A. Yuniarto, and T. Hadibarata, "Adsorption of Basic Dyes Crystal Violet on Agricultural Biomass : Characterization, Isotherm and Kinetic Studies," *Int. J. Integr. Eng.*, vol. 14, no. 1, pp. 269–275, 2022, doi: https://doi.org/10.30880/ijie.2022.14.01.025.

[11] R. I. Arvianto, K. Mauludi, A. K. Damayanti, and M. F. Pradipta, "Studi Kinetika Adsorpsi Emas Menggunakan Kulit Mangga (Mangifera indica) Termodifikasi Asam Sulfat," *Chim. Nat. Acta*, vol. 7, no. 1, pp. 1–6, 2019, doi: https://doi.org/10.24198/cna.v7.n1.19191.

[12] U. O. Aigbe, R. Maluleke, T. C. Lebepe, O. S. Oluwafemi, and O. A. Osibote, "Rhodamine 6G Dye Adsorption Using Magnetic Nanoparticles Synthesized With the Support of Vernonia Amygdalina Leaf Extract (Bitter Leaf)," *J. Inorg. Organomet. Polym. Mater.*, vol. 33, pp. 4012–4031, 2023, doi: 10.1007/s10904-023-02639-3.

[13] Jefri, N. A. Fithri, and N. Ramadhan, "Enhanced Selectivity of Ni/Al LDH for Cationic Dye Adsorption via Gambier Leaf Extract Modification," *Indones. J. Mater. Res.*, vol. 3, no. 1, pp. 1–7, 2025, doi: https://doi.org/10.26554/ijmr.20253148.

[14] S. I. Manalu and S. B. Etika, "Pengaruh pH dan Waktu Kontak Adsorpsi Rhodamin B terhadap Ekstrak Pelat Flavonoid dari Kulit Rambutan(Nephelium lappaceum)," *J. Pendidik. dan Sains*, vol. 5, no. 4, pp. 1942–1953, 2025, doi: https://doi.org/10.58578/masaliq.v5i4.6744.

[15] Sridevitri and S. B. Etika, "Optimasi pH dan Waktu Kontak dalam Adsorpsi Metylene Blue dengan Ekstrak Kulit Rambutan," *Masal. J. Pendidik. dan Sains*, vol. 5, no. 4, pp. 2001–2014, 2025, doi: https://doi.org/10.58578/masaliq.v5i4.6822.

[16] L. Luqyana Z. T. M and P. Husni, "Aktivasi Farmakologi Tanaman Mangga (Mangifera Indica L.)," *Farmaka*, vol. 17, no. 2, pp. 187–194, 2019, doi: https://doi.org/10.24198/jf.v17i2.21994.

[17] O. D. Anggraini, "Efek Ekstrak Kulit Mangga Arumanis terhadap Penurunan Edema Kaki Mencit Putih Jantan yang Diinduksi Karagenin," *Skripsi*, 2016.

[18] Y. Noviyanty, W. Ardelia, and Hepiyansori, "Penetapan Kadar Senyawa Flavonoid Total dari Ekstrak Etanol Kulit Buah Mangga Arum Manis (Mangifera Indica L. Var. Arum Manis) dengan Metode Spektrofotometri Uv-Vis," *J. Sains Kesehat.*, vol. 29, no. 1, pp. 1–8, 2022, doi: https://doi.org/10.37638/jsk.29.1.1-8.

[19] I. Ifmaily, B. A. Martinus, and A. Rahmawati, "Uji Aktivitas Antioksidan Ekstrak Kulit Buah Mangga Arumanis (Mangifera Indica L .) dengan Metode DPPH Serta Uji Toksisitasnya," *J. Vent.*, vol. 2, no. 3, pp. 392–399, 2024, doi: https://doi.org/10.59680/ventilator.v2i3.1438.

[20] H. Kim *et al.*, "Antioxidant and Antiproliferative Activities of Mango (Mangifera indica L .) Flesh and Peel," *Food Chem.*, vol. 121, pp. 429–436, 2010, doi: 10.1016/j.foodchem.2009.12.060.

[21] Badan Pusat Statistik, *Statistik Hortikultura 2024*. 2025.

[22] S. Dutta, B. Gupta, S. K. Srivastava, and A. K. Gupta, "Recent Advances On the Removal of Dyes from Wastewater Using Various Adsorbents: A Critical Review," *Mater. Adv.*, vol. 2, pp. 4497–4531, 2021, doi: 10.1039/d1ma00354b.

[23] S. R. Patra and S. P. Mishra, "Insights Into the Properties and Role of Mangifera indica (Mango) Peel

in Decontamination of Wastewater," *Sustain. Environ.*, vol. 11, no. 1, pp. 1–24, 2025, doi: 10.1080/27658511.2025.2533572.

[24] A. Nugroho, N. L. Amanah, and R. G. Firdaus, "Adsorption Study of Mango Peel Activated Carbon as Iron Removal for Batik Waste Industry," *J. Rekayasa Proses*, vol. 16, no. 1, pp. 19–24, 2022, doi: 10.22146/jrekpros.69404.

[25] F. Mas'ud, "Kajian Potensi Kulit Buah Mangga Sebagai Bahan Pangan," *Agritechno*, vol. 16, no. 01, pp. 13–18, 2023, doi: https://doi.org/10.20956/at.v16i1.1008.

[26] Y. Noviyanty, Hepiyansori, and F. Afriyanto, "Profil Fitokimia dari Ekstrak Etanol Kulit Buah Mangga Arum Manis (Mangifera Indica L.)," *J. Ilm. Farm.*, vol. 7, no. 2, pp. 242–255, 2020, doi: https://doi.org/10.52161/jiphar.v7i2.183.

[27] V. J. Anggraeni, S. Yulianti, and R. S. Panjaitan, "Artikel Review: Fitokimia dan Aktivitas Antibakteri dari Tanaman Mangga (Mangifera indica L)," *Indones. Nat. Res. Pharm. J.*, vol. 5, no. 2, pp. 102–113, 2020, doi: https://doi.org/10.5281/zenodo.7545893.

[28] R. Y. Asworo and H. Widwiastuti, "Pengaruh Ukuran Serbuk Simplisia dan Waktu Maserasi terhadap Aktivitas Antioksidan Ekstrak Kulit Sirsak," *Indones. J. Pharm. Educ.*, vol. 3, no. 2, pp. 256–263, 2023, doi: 10.37311/ijpe.v3i2.19906.

[29] F. Setyaningum, D. Raharjo, and N. Luthfiyanti, "Pengaruh Pelarut terhadap Flavonoid Total, Fenolik Total dan Aktivitas Antioksidan Daun Kunyit (Curcuma Longa L) dengan Metode ABTS," *J. Kesehat. Tambusai*, vol. 6, no. 3, pp. 12465–12476, 2025, doi: https://doi.org/10.31004/jkt.v6i3.50198.

[30] R. Sari, L. Pratiwi, and P. Apridamayanti, "Efektivitas SNEDDS Ekstrak Kulit Manggis Terhadap Bakteri P. mirabilis dan S. epidermidis yang Terdapat pada Ulkus Diabetik," *Pharm Sci Res*, vol. 3, no. 3, pp. 130–138, 2016, doi: https://doi.org/10.7454/psr.v3i3.3287.

[31] Q. W. Zhang, L. G. Lin, and W. C. Ye, "Techniques for Extraction and Isolation of Natural Products: A Comprehensive Review," *Chin. Med.*, vol. 13, no. 20, pp. 1–26, 2018, doi: 10.1186/s13020-018-0177-x.

[32] M. A. Azis, T. S. Wardani, and A. Fitriawati, "Uji Aktivitas Antibakteri Ekstrak dan Fraksi n-Heksan, Etil Asetat, Air Kulit Buah Naga Putih (Hylocereus Undatus) Terhadap Staphylococcus Epidermidis ATCC 12238," *J. Ris. Ilmu Farm. dan Kesehat.*, vol. 2, no. 4, pp. 41–56, 2024, doi: https://doi.org/10.61132/obat.v2i4.478.

[33] I. A. Ibrahim, H. M. M. Ebeid, Y. A. E.-R. Heikal, and H. M. Elhariry, "Sustainable Valorization of Mango Peel Waste by Extracting Bioactive Compounds for Functional Applications," *Nat. Res.*, pp. 1–44, 2025, doi: https://doi.org/10.1038/s41598-025-28141-z.

[34] S. Kainth, P. Sharma, and O. P. Pandey, "Green Sorbents from Agricultural Wastes : A Review of Sustainable Adsorption Materials," *Appl. Surf. Sci. Adv.*, vol. 19, no. 100562, pp. 1–21, 2024, doi: 10.1016/j.apsadv.2023.100562.

[35] B. K. Nandi, A. Goswami, and M. . Purkait, "Adsorption Characteristics of Brilliant Green Dye on Kaolin," *J. Hazard. Mater.*, vol. 161, pp. 387–395, 2009, doi: 10.1016/j.jhazmat.2008.03.110.

[36] A. Daouda, A. T. Honorine, N. G. Bertrand, and D. Richard, "Adsorption of Rhodamine B onto Orange Peel Powder," *Am. J. Chem. 2019, 9(5) 142-149 DOI*, vol. 9, no. 5, pp. 142–149, 2019, doi: 10.5923/j.chemistry.20190905.02.

[37] S. Chang *et al.*, "Efficient Adsorption of Rhodamine B Using Synthesized Mg–Al Hydrotalcite/Sodium Carboxymethylcellulose/ Sodium Alginate Hydrogel Spheres : Performance and Mechanistic Analysis," *Heliyon*, vol. 10, no. 9, 2024, doi: 10.1016/j.heliyon.2024.e30345.

[38] A. A. Oyekanmi, A. Ahmad, K. Hossain, and M. Rafatullah, "Adsorption of Rhodamine B Dye from Aqueous Solution onto Acid Treated Banana Peel : Response Surface Methodology, Kinetics and Isotherm Studies," *PLoS One*, vol. 14, no. 5, pp. 1–20, 2019, doi: https://doi.org/10.1371/journal. pone.0216878.

[39] A. Strebel, M. Behringer, H. Hilbig, A. Machner, and B. Helmreich, "Anionic Azo Dyes and Their Removal from Textile Wastewater Through Adsorption by Various Adsorbents : A Critical Review," *Environ. Eng.*, pp. 1–17, 2024, doi: 10.3389/fenve.2024.1347981.

[40] A. Thakur and H. Kaur, "Response Surface Optimization of Rhodamine B Dye Removal Using Paper Industry Waste as Adsorbent," *Int. J. Ind. Chem.*, vol. 8, no. 2, pp. 175–186, 2017, doi: 10.1007/s40090-017-0113-4.

[41] T. C. Caglar and B. Kayranli, "Comparative Evaluation of Regeneration Strategies for Rhodamine B Removal Using Raw Date Seeds : Insights into Adsorption Mechanisms," *ACS Omega*, 2026, doi: 10.1021/acsomega.6c01845.

[42] D. Nayeri and S. A. Mousavi, "Dye Removal from Water and Wastewater by Nanosized Metal Oxides - Modified Activated Carbon : A Review on Recent Researches," *J. Environ. Heal. Sci. Eng.*, vol. 18, pp. 1671–1689, 2020, doi: https://doi.org/10.1007/s40201-020-00566-w.

[43] K. Y. Foo and B. H. Hameed, "Insights Into the Modeling of Adsorption Isotherm Systems," *Chem. Eng. J. J.*, vol. 156, pp. 2–10, 2010, doi: 10.1016/j.cej.2009.09.013.

[44] N. Ayawei, A. N. Ebelegi, and D. Wankasi, "Modelling and Interpretation of Adsorption Isotherms," *J. Chem.*, pp. 1–11, 2017, doi: https://doi.org/10.1155/2017/3039817.

[45] D. A.O, O. A.P, and O. A.M, "Langmuir , Freundlich , Temkin and Dubinin – Radushkevich Isotherms Studies of Equilibrium Sorption of Zn2+ Unto Phosphoric Acid Modified Rice Husk," *IOSR J. Appl. Chem.*, vol. 3, no. 1, pp. 38–45, 2012, doi: https://doi.org/10.9790/5736-0313845.

[46] G. Annadurai, R. Juang, and D. Lee, "Use of Cellulose-Based Wastes for Adsorption of Dyes from Aqueous Solutions," *J. Hazard. Mater. B92*, vol. 92, pp. 263–274, 2002, doi: https://doi.org/10.1016/S0304-3894(02)00017-1.

[47] D. T. C. Nguyen, T. Van Tran, P. S. Kumar, A. T. M. Din, A. A. Jalil, and D.-V. Vo, "Invasive Plants as Biosorbents for Environmental Remediation : a Review," *Environ. Chem. Lett.*, vol. 20, pp. 1421–1451, 2022, doi: 10.1007/s10311-021-01377-7.

[48] K. . Tan and B. . Hameed, “Insight into the Adsorption Kinetics Models for the Removal of Contaminants from Aqueous Solutions,” *J. Taiwan Inst. Chem. Eng.*, vol. 74, pp. 25–48, 2017, doi: 10.1016/j.jtice.2017.01.024.

[49] Q. Hu, S. Pang, and D. Wang, “In-depth Insights into Mathematical Characteristics, Selection Criteria and Common Mistakes of Adsorption Kinetic Models: A Critical Review,” *Sep. Purif. Rev.*, vol. 00, no. 00, pp. 1–19, 2021, doi: 10.1080/15422119.2021.1922444.

[50] A. Kanwal, R. Rehman, M. Imran, and G. Samin, “Phytoremediative adsorption methodologies to decontaminate water from dyes and organic pollutants,” *R. Soc. Chem.*, vol. 13, pp. 26455–26474, 2023, doi: 10.1039/d3ra02104a.

[51] A. Solinska, J. Marchewka, M. Sitarz, and T. Bajda, “Infrared Spectroscopy : the Key to Elucidating the Sorption Mechanism of Surfactants, Dyes and Pharmaceuticals on Mineral Composite Material,” *Spectrochim. Acta Part A Mol. Biomol. Spectrosc. J.*, vol. 122758, pp. 1–10, 2023, doi: 10.1016/j.saa.2023.122758.